The Astrophysical Journal, 720:173–177, 2010 September 1 doi:10.1088/0004-637X/720/1/173

GAS-PHASE REACTIONS OF HYDRIDE ANION, H^-

Oscar Martinez Jr.[1], Zhibo Yang[1], Nicholas J. Demarais[1], Theodore P. Snow[2,3], and Veronica M. Bierbaum[1,3]
[1] Department of Chemistry and Biochemistry, 215 UCB, University of Colorado, Boulder, CO 80309-0215, USA;
Oscar.Martinez@colorado.edu, Zhibo.Yang@colorado.edu, Nicholas.Demarais@colorado.edu, Veronica.Bierbaum@colorado.edu
[2] Department of Astrophysical and Planetary Sciences, 391 UCB, University of Colorado, Boulder, CO 80309-0391, USA; Theodore.Snow@colorado.edu
[3] Center for Astrophysics and Space Astronomy, 389 UCB, University of Colorado, Boulder, CO 80309-0389, USA
Received 2010 June 3; accepted 2010 June 28; published 2010 August 6

ABSTRACT

Rate constants were measured at 300 K for the reactions of the hydride anion, H^-, with neutral molecules C_2H_2, H_2O, CH_3CN, CH_3OH, $(CH_3)_2CO$, CH_3CHO, N_2O, CO_2, O_2, CO, CH_3Cl, $(CH_3)_3CCl$, $(CH_3CH_2)_2O$, C_6H_6, and D_2 using a flowing-afterglow instrument. Experimental work was supplemented by ab initio calculations to provide insight into the viability of reaction pathways. Our reported rate constants should prove useful to models of astrophysical environments where conditions prevail for the existence of both H^- and neutral species. The variety of neutral reactants studied includes representative species from prototypical chemical groups, effectively mapping reactivity trends for the hydride anion.

Key words: astrochemistry – ISM: clouds – ISM: molecules – methods: laboratory – molecular processes

1. INTRODUCTION

The anion of the hydrogen atom, though seemingly simple, has drawn much attention because of its involvement in many reactions important to our understanding of cosmology and astrophysics. Hydride, H^-, has been implicated in the formation of H_2, the first coolant available to the universe for seeding star and galaxy formation after the big bang (cf. Glover et al. 2006). Our experimental studies recently contributed to early universe models by remeasuring and refining an older measurement of the reaction rate constant for the associative-detachment (AD) reaction $H + H^- \longrightarrow H_2 + e^-$ (Fehsenfeld et al. 1973; Schmeltekopf et al. 1967; Martinez et al. 2009).

Although detection of H^- in astrophysical environments remains elusive (Ross et al. 2008), a firm acceptance of its presence exists. The hydride ion has been correlated to the opacity of the Sun and other late-type stars (Wildt 1939; Chandrasekhar 1944; Münch 1945; Chandrasekhar & Breen 1946). Additionally, there is support for the prediction of H^- in regions of the interstellar medium such as in the transition zones of planetary nebulae (Black 1978), where the population of neutral hydrogen and free electrons suggests the existence of H^-, or in photodissociation regions and dark clouds. Field (2000) proposed a model suggesting hydride may also be involved in H_2 formation, again via an AD process similar to the one that was important in the early universe. However, in this case, H^- production occurs on the surface of dust grains with weakly bound surface electrons rather than by direct electron capture by hydrogen atoms.

A variety of the regions with likely presence of H^- overlap molecular regions at their boundaries. An assorted range of chemical processes can be expected because of the reactivity of the hydride anion. Thus, an understanding of this reactivity should reveal the degree to which H^- drives astrophysical processes. Neutral reactants employed in this study were chosen to map the chemistry of H^- with representatives from prototypical groups of compounds. Eleven of the compounds studied (C_2H_2, H_2O, CH_3CN, CH_3OH, $(CH_3)_2CO$, CH_3CHO, N_2O, CO_2, O_2, CO, and C_6H_6) have been detected in the interstellar medium (ISM).

Previously measured rate constants for H^- with neutral molecules (C_2H_2, H_2O, CH_3CN, N_2O, O_2, CO, CH_3Cl, and C_6H_6) were determined decades ago to test ion-molecule collision models. For references, see the footnotes to Table 1. Only the rate constant for $H^- + H_2O$ has been studied by more than one laboratory. Here, we increase the number and source of existing measurements and contribute seven previously unmeasured reaction rate constants of H^- with the molecules CH_3OH, $(CH_3)_2CO$, CH_3CHO, CO_2, $(CH_3)_3CCl$, $(CH_3CH_2)_2O$, and D_2.

A majority of these reactions exhibit proton-transfer mechanisms, illustrating the basicity of the hydride ion. In contrast, reactions with non-acidic neutrals occur by AD, atom transfer, addition, substitution, or elimination channels. Reaction efficiencies are strongly correlated with the potential energy surface along the reaction coordinate. Ab initio calculations provide an insight into the reaction mechanisms and their relation to reaction efficiencies.

2. EXPERIMENTAL METHODS

Experiments were carried out using a flowing-afterglow instrument at the University of Colorado at Boulder. Details of the instrument and method can be found elsewhere (Bierbaum 2003; Van Doren et al. 1987). Briefly, ions are formed and then carried downstream in a known flow of helium buffer gas (99.99%; further purified by flowing through a molecular sieve trap immersed in liquid nitrogen) to a reaction region. In this case, H^- is formed by electron ionization (70 eV ionization energy) on a trace amount of ammonia gas (NH_3, Air Products and Chemicals Inc., 99.99%) via the dissociative attachment process $NH_3 + e^- \longrightarrow H^- + NH_2$ (cf. Martinez et al. 2009). Ions are formed in low density using 1–2 μA emission current to ensure the existence of free diffusion. Sufficient concentration of NH_3 was used to ensure that hydride formation (ionization) was complete before the reaction region. Additionally, ions are thermalized by $\sim 10^4$ collisions with the helium carrier gas (pressure = 0.5 Torr; flow = 220 std cm^3 s^{-1}). The reaction region is a flow tube (41.85 cm^2) with seven inlets at fixed distances for the addition of neutral reagents. A measured amount of reactant is added, and the decrease of the reactant-ion signal is monitored as a function of reaction distance by a quadrupole mass filter coupled to an electron multiplier. Reactions are carried out under pseudo first-order conditions and standard kinetic analysis is used to determine rate constants. The neutral reagents are acetylene (C_2H_2; $\geqslant$

Table 1
Hydride/Neutral Molecule Reactions

Neutral Reactant	Product	k_{exp}[a] (10^{-9} cm^3 s^{-1})	k_{col}[b] (10^{-9} cm^3 s^{-1})	Efficiency (k_{exp}/k_{col})	Literature Values (10^{-9} cm^3 s^{-1})	ΔH^c_{exp} (kcal mol^{-1})	$\Delta H^d_{theor(0\ K)}$ (kcal mol^{-1})	$\Delta H^{d,e}_{theor(298\ K)}$ (kcal mol^{-1})
			Proton Abstraction Reactions					
C_2H_2	$C_2H^- + H_2$	3.1 ± 0.3	4.44	0.70	$4.42^f \pm 25\%$	−21.6	−26.2	−24.1
H_2O[g]	$OH^- + H_2$	4.8 ± 1.1	9.18	0.61	$3.8^h \pm 30\%$, $3.7^i \pm 25\%$	−10.3	−14.3	−12.5
CH_3CN	$CH_2CN^- + H_2$	11 ± 1	18.5	0.57	$13^j \pm 2$ ($\pm 25\%$)	−26.3	−27.2	−25.1
CH_3OH	$CH_3O^- + H_2$	6.1 ± 0.8	9.3	0.66	N/A	−18.6	−21.3	−19.5
$(CH_3)_2CO$	$CH_3COCH_2^- + H_2$	7.0 ± 0.8	14.9	0.47	N/A	−31.8	−33.1	−31.5
CH_3CHO	$CH_2CHO^- + H_2$	6.4 ± 1.1	1.39	0.51	N/A	−34.9	−35.9	−34.0
			Atom Abstraction/Addition Reactions					
N_2O	$OH^- + N_2$	1.0 ± 0.1	4.27	0.23	$1.1^k \pm 0.3$	−87.7	−89.2	−87.4
CO_2	HCO_2^-	0.09 ± 0.02	4.03	0.022	N/A	−50.9	−52.2	−52.0
			Associative Detachment Reactions					
O_2	$HO_2 + e^-$	1.4 ± 0.1	2.97	0.46	1.2^k ($\pm 20\%$)	−34.2	-30.3^l	-29.4^l
CO	$CHO + e^-$	0.020 ± 0.008	3.76	0.007	$\cong 0.05^k$	2.1	−1.2	−0.9
			S_N2/E2 Reactions					
CH_3Cl	$Cl^- + CH_4$	2.5 ± 0.1	10.7	0.23	$3.0^m \pm 0.2$ ($\pm 20\%$)	−85.0	−91.4	−91.5
$(CH_3)_3CCl$	$Cl^- + H_2 + (CH_3)_2CCH_2$	4.0 ± 0.5	13.4	0.32	N/A	−76.2	−77.5	−78.0
			No Reaction					
$(CH_3CH_2)_2O$	$H_2 + C_2H_5O^- + C_2H_4$	N/A	7.2	N/A	N/A	−5.2	−6.2	−3.5
C_6H_6	$C_6H_5^- + H_2$	Slow	7.55	N/A	$>0.05^n$	1.1	−2.5	−0.5
D_2	$D^- + HD$	<0.01	2.33	N/A	N/A	0.9	1.1	1.1

Notes.
[a] Error represents 1σ of the mean of the experimental measurements. There is an additional systematic error of $\pm 20\%$.
[b] k_{col} is determined according to Langevin theory for reactions involving neutral species having no dipole moment and parameterized trajectory theory for those reactions involving neutral species with dipole moments.
[c] Values determined using additivity methods with experimental values for ionization energies, bond energies, electron affinities, and heats of formation taken from Linstrom & Mallard (2010).
[d] MP2(full)/aug-cc-pVDZ theory level including zero-point energy corrections.
[e] Including thermal energy corrections at 298 K.
[f] Mackay et al. (1977).
[g] Stockdale et al. (1969) reported an unreasonably high value of $540 \pm 160 \times 10^{-9}$ cm^3 s^{-1}.
[h] Melton & Neece (1971).
[i] Betowski et al. (1975).
[j] Mackay et al. (1976).
[k] Dunkin et al. (1970).
[l] CCSD(T)/aug-cc-pVTZ//MP2(full)/aug-cc-pVDZ theory level including zero-point energy corrections.
[m] Tanaka et al. (1976).
[n] Bohme & Young (1971).

99.6%), water (H_2O; deionized), acetone ($(CH_3)_2CO$; $\geqslant$ 99.5%), acetonitrile (methyl cyanide; CH_3CN; 99.8%), methanol (CH_3OH; $\geqslant$ 99.9), acetaldehyde (CH_3CHO; $\geqslant$ 99.5%), nitrous oxide (N_2O; 99.0%), carbon dioxide (CO_2; $\geqslant$ 99%), oxygen (O_2; $\geqslant$ 99.994%), carbon monoxide (CO; 99.5%), methyl chloride (CH_3Cl; 99.5%), *tert*-butyl chloride ($(CH_3)_3CCl$; $\geqslant$ 99.5%), diethyl ether ($(CH_3CH_2)_2O$; 99.9%), benzene (C_6H_6; $\geqslant$ 99.9%), and deuterium (D_2; $\geqslant$ 99.8%).

3. RESULTS AND DISCUSSION

Table 1 summarizes our results for all reactions, including reaction rate constants, collisional rate constants, efficiencies, prior literature values, and exothermicities. We observe a wide range of rate constants and their resulting efficiencies. Here, theoretical calculations serve to explore reaction mechanisms and identify those that are viable. In this work, we report a systematic error of $\pm 20\%$, based on the accuracy of experimental quantities that are used in determining our rate constant measurements. Furthermore, reaction rate constants are reported with error bars representing 1σ of the mean, an indication of the precision of our measurements. Our reported rate constant values in the text are followed by the total number of rate constant measurements for each reaction. We report an efficiency as k_{exp}/k_{col}, where k_{col} is the collisional rate constant determined by Langevin theory (Gioumousis & Stevenson 1958) for reactions involving neutral species without a dipole moment (C_2H_2, $(CH_3CH_2)_2O$, CO_2, O_2, C_6H_6, and D_2) and by parameterized trajectory theory (Su & Chesnavich 1982) for those reactions involving neutral species with dipole moments (H_2O, CH_3CN, CH_3OH, $(CH_3)_2CO$, N_2O, CH_3CHO, CO, CH_3Cl and $(CH_3)_3CCl$). Values for dipole moments and polarizabilities were taken either from the experimental thermochemical data portion of the NIST Computational Chemistry Comparison and Benchmark Database (CCCBD 2010) or from the 89th edition of the CRC Handbook of Chemistry and Physics (Lide 2008).

Enthalpies of reaction, reported in Table 1 as ΔH_{exp}, have been determined using additivity methods with values for ionization energies, bond energies, electron affinities, and heats of formation taken from the NIST Chemistry WebBook

(Linstrom & Mallard 2010) and the CRC Handbook of Chemistry and Physics. For comparison, enthalpies were also determined using ab initio calculations; these values are reported at both absolute zero and 298 K. Structures and energies of anions and neutral species were determined using *Gaussian 03* (Frisch et al. 2004) at the MP2(full)/aug-cc-pVDZ level of theory. Enthalpies resulting from additivity methods and calculated enthalpy determinations are in excellent agreement.

Experimental difficulties arise when we quantitatively compare ion intensities to determine product branching ratios. Mass discrimination, the transmission of different-mass ions with different efficiencies through the detection region, manifests to a significant degree with hydride studies because of the sizable range of masses of ions monitored simultaneously. Moreover, secondary ion chemistry can occur. Although mass discrimination can make it a challenge to account for 100% conversion of a reactant ion into products, one can make reasonable assumptions to understand the reactive pathways involved. Where applicable, we have noted other possible channels of a reaction based on calculated reaction enthalpies and ab initio calculations. However, we do not present quantitative branching ratio determinations.

For discussion, reactions have been categorized into five groups based on reaction mechanism. These mechanisms include proton abstraction, atom abstraction or addition reactions, AD, substitution (S_N2)/elimination (E2), and a final group where reactions were not observed.

3.1. Proton Abstraction

The neutral reagents C_2H_2, H_2O, CH_3CN, CH_3OH, $(CH_3)_2CO$, and CH_3CHO react with H^- to form H_2 via RH + $H^- \longrightarrow R^- + H_2$. Such proton abstraction reactions have relatively large rate constants ranging from 3.1 to 11 $\times$ 10^{-9} cm^3 s^{-1}. Similarly, reaction efficiencies, while not at 100%, are generally higher than other reactions in this study.

Mackay et al. (1977) measured the rate constant for the proton transfer reaction of hydride with acetylene with a flowing-afterglow instrument in a manner similar to ours and reported $k = 4.42 \pm 25\% \times 10^{-9}$ cm^3 s^{-1}. In comparison, our measured rate constant is $3.1 \pm 0.3 \times 10^{-9}$ cm^3 s^{-1} (15 measurements). Because of the rapid reaction between hydride and acetone, as shown below, we worked to eliminate contamination from this reaction in the rate constant measurement of H^- with acetylene. Based on calculations and careful experiments, we conclude that an insignificant amount of acetone is present at reaction. Our rate constant measurements overlap with the previously measured rate constant of Mackay et al. within our combined error bars.

The reaction of hydride with water is the only reaction in this study for which more than one rate constant measurement has been reported. Betowski et al. (1975) determined a rate constant of $3.7 \pm 25\% \times 10^{-9}$ cm^3 s^{-1} from four experimental measurements for the reaction $H^- + H_2O \longrightarrow OH^- + H_2$ at 297 K using a flowing-afterglow technique. Melton & Neece (1971) carried out an energy-variable study for this reaction ranging from 0 to 10 eV and reported a value of $3.8 \pm 30\% \times 10^{-9}$ cm^3 s^{-1} (0 eV) using a mass spectrometric technique. An earlier measurement from Stockdale et al. (1968, 1969) for the same reaction was reported as $5.4 \pm 1.6 \times 10^{-7}$ cm^3 s^{-1}. Rate constants by Stockdale et al. were measured using a pulsed-source time-of-flight mass spectrometer, and their reported rate constant measurement at 0 eV ion energy (i.e., $E_{lab}(H^-)$) exceeds the collision rate constant by a factor of 60 and is therefore not physically reasonable. Our determination of this reaction rate constant is $4.8 \pm 1.1 \times 10^{-9}$ cm^3 s^{-1} (19 measurements). The experimental conditions of our study are most similar to those of Betowski et al. where ions were produced using a similar method (i.e., electron ionization on a precursor) and subsequently thermalized via collisions with carrier gas molecules.

Mackay et al. (1976) reported a rate constant of $13 \pm 2 \times 10^{-9}$ cm^3 s^{-1} (mean value and precision of eight measurements, with an overall accuracy of $\pm 25\%$) for the reaction of hydride with CH_3CN. The measurement was made using a flowing-afterglow instrument under conditions similar to ours. Our reported measurement, $11 \pm 1 \times 10^{-9}$ cm^3 s^{-1} (10 measurements), is within the error bars of the former measurement, when systematic errors are included. As with the data of Mackay et al., we saw no evidence of nucleophilic displacement, $H^- + CH_3CN \longrightarrow CN^- + CH_4$, even though additivity methods indicate that the reaction is exothermic, $\Delta H = -53.0$ kcal mol^{-1}. In fact, calculations indicate that nucleophilic displacement by the hydride anion has a transition-state barrier above the total energy of the reactants by 15.1 kcal mol^{-1}.

We report a rate constant for the proton transfer reaction of methanol with hydride as $6.1 \pm 0.8 \times 10^{-9}$ cm^3 s^{-1} (12 measurements). Although a substitution mechanism for the methanol/hydride reaction producing OH^- and CH_4 is more exothermic ($\Delta H = -37.0$ kcal mol^{-1} versus -18.6 kcal mol^{-1} for the proton-transfer mechanism), calculations predict a high transition-state energy barrier of 13.2 kcal mol^{-1} along the reaction coordinate that effectively prohibits this reaction.

Our measured rate constant for the reaction of hydride with acetone, $7.0 \pm 0.8 \times 10^{-9}$ cm^3 s^{-1} (10 measurements), indicates a rather rapid reaction. Our measurement for the rate constant of hydride with acetaldehyde is $6.4 \pm 1.1 \times 10^{-9}$ cm^3 s^{-1} (nine measurements). There are no previous studies of these reactions.

3.2. Atom Abstraction/Addition

Reaction rate constants and efficiencies for the reactions of H^- with N_2O and CO_2 are markedly different than those of proton-transfer reactions, as shown in Table 1. The reaction coordinate plot of H^- with N_2O is shown in Figure 1, with all energies relative to the total energy of the reactants. The most viable pathway, attack of H^- on the terminal nitrogen atom, leads to the formation of an association intermediate that is more stable than the reactants by -45.7 kcal mol^{-1}. From the intermediate, an AD path is endothermic by 17.1 kcal mol^{-1} and does not occur; however, the reactants can proceed through a transition state at -20.6 kcal mol^{-1} along the dissociation path and on to a dissociation intermediate (93.0 kcal mol^{-1} lower in energy than reactants). Similarly, direct attack on the oxygen atom leads to an association intermediate then transition state -4.2 kcal mol^{-1} and -0.2 kcal mol^{-1} lower in energy than the reactants, respectively. This transition state then proceeds to the dissociation intermediate described above. Dunkin et al. measured the reactivity of hydride with nitrous oxide and reported a rate constant of $1.1 \pm 0.3 \times 10^{-9}$ cm^3 s^{-1}, in agreement with our measurement of $1.0 \pm 0.1 \times 10^{-9}$ cm^3 s^{-1} (seven measurements).

For the reaction of H^- with CO_2, four channels were investigated. Figure 2(a) shows the hydrogen atom attacking an oxygen atom of CO_2. The AD and oxygen abstraction channels that would result from this attack are hampered by a transition state 8.9 kcal mol^{-1} above the energy of the reactants. Alternately, Figure 2(b) shows the hydrogen atom attacking the carbon atom of the CO_2 and forming a reactant intermediate

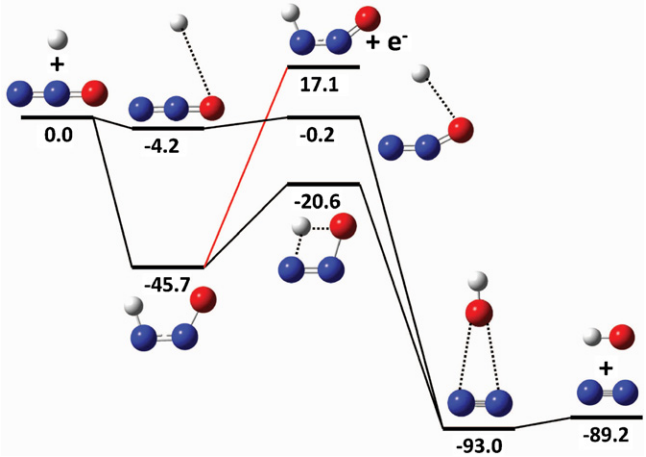

Figure 1. H^- + N_2O reaction coordinate plot. Energies obtained from calculations performed at the MP2(full)/aug-cc-pVDZ level of theory (kcal mol^{-1}).

-52.2 kcal mol^{-1} lower in energy than the reactants. The AD channel producing the neutral product with the hydrogen bound to the carbon does not occur; the reaction is endothermic with the products 33.9 kcal mol^{-1} above the reactants. The atom-transfer reaction forming CO and HO^- from the reactant intermediate has a transition-state barrier 9.7 kcal mol^{-1} higher in energy than the reactants and also does not occur. Reaction of H^- with CO_2 is slow. Our measured rate constant is $0.09 \pm 0.02 \times 10^{-9}$ cm^3 s^{-1} (six measurements). Evidence of trace formation of the HCO_2^- species described in Figure 2(b) is seen, indicating the process is third order (He reaction flow tube pressure = 450 mTorr). Reaction in the interstellar medium, however, may occur by radiative association.

3.3. Associative Detachment

Hydride reacts with molecular oxygen (O_2) and carbon monoxide (CO) via AD reactions. Similar to the proton-transfer reactions discussed previously, these reactions proceed without barriers along the approach of reactants. A large difference is evident, however, when we compare efficiencies and rate constants for these reactions, as shown in Table 1. The differences are attributed to relative enthalpies; whereas the AD channel for the O_2 reaction is exothermic ($\Delta H = -34.2$ kcal mol^{-1}), the CO reaction is essentially thermoneutral (2.1 kcal mol^{-1}). Additionally, we found that MP2 enthalpy calculations underestimate values for this channel by ~9 kcal mol^{-1} relative to the experimental values. Better agreement was found using the CCSD(T)/aug-cc-pVTZ//MP2(full)/aug-cc-pVDZ level of theory.

Dunkin et al. (1970), in clarifying the electron affinity of O_2, measured a rate constant of $1.2 \pm 20\% \times 10^{-9}$ cm^3 s^{-1} for the H^- + O_2 reaction. Our AD reaction used a flowing afterglow with conditions similar to theirs. Our value, $1.4 \pm 0.1 \times 10^{-9}$ cm^3 s^{-1} (eight measurements), is in good agreement with their published value.

Dunkin et al. also determined the reaction products and considered formation of O_2^- + H, OH^- + O, and O^- + OH. Hydroxide formation seemed plausible since this reaction is exothermic by 8.6 kcal mol^{-1}. O^- formation, however, is thermoneutral (0.4 kcal mol^{-1}) and cannot compete with AD. Charge transfer is endothermic by 7.0 kcal mol^{-1} and should therefore not occur. A careful experimental search for these alternative products turned out negative, implying that if these reactions occur, they have less than 1% of the AD rate. Similarly, our studies show clear evidence of the AD channel. However, the presence of background OH^- in our spectra prevents quantitative branching-ratio determination for relatively minor channels.

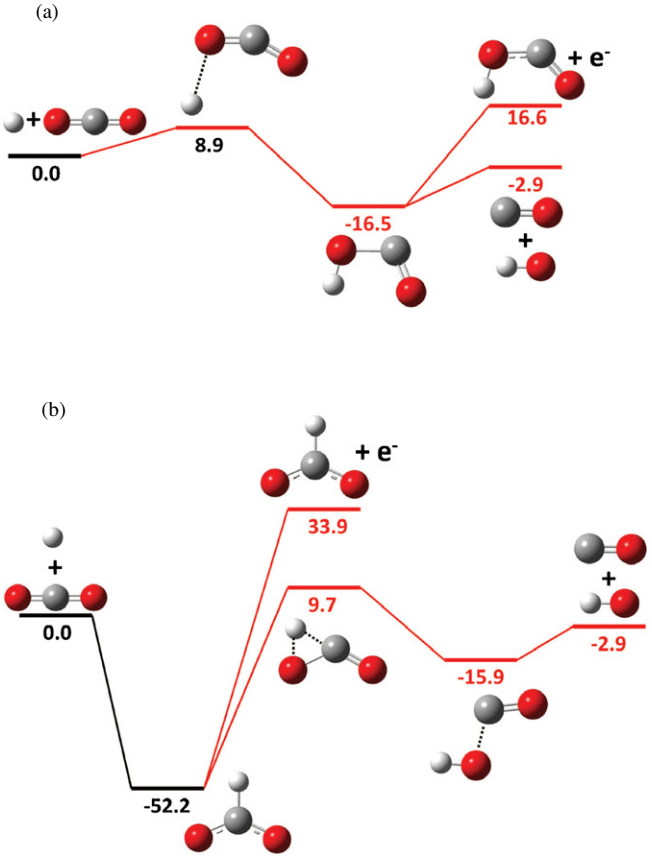

Figure 2. (a) H^- + CO_2 reaction coordinate plot (H atom attacking oxygen of CO_2). (b) H^- + CO_2 reaction coordinate plot (H atom attacking carbon of CO_2). Energies obtained from calculations performed at the MP2(full)/aug-cc-pVDZ level of theory (kcal mol^{-1}).

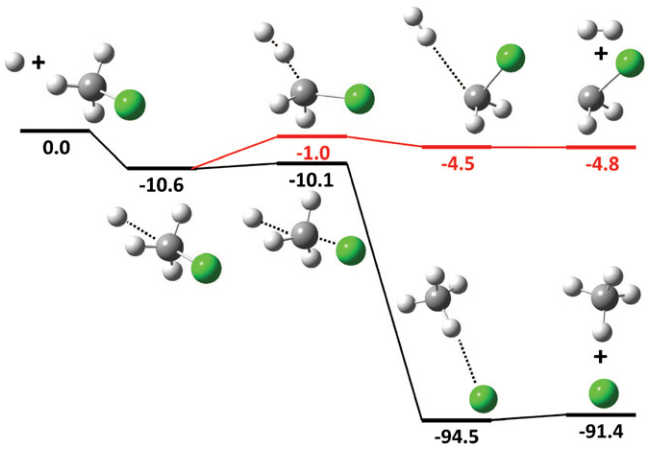

Figure 3. H^- + CH_3Cl reaction coordinate plot. Energies obtained from calculations performed at the MP2(full)/aug-cc-pVDZ level of theory (kcal mol^{-1}).

Our determination of the rate constant for hydride reacting with CO is $2.0 \pm 0.8 \times 10^{-11}$ cm^3 s^{-1} (eight measurements) and AD is the only channel. Our result is smaller than the previously published value of $\sim 5.0 \times 10^{-11}$ cm^3 s^{-1}. However, the large error bars reflect considerable variation in our measurements. Influence of the thermoneutrality of the reaction of H^- with CO manifests itself in the low reaction rate constant.

3.4. $S_N2/E2$ Reactions

Hydride reactivity with methyl chloride proceeds via a substitution mechanism, and reaction with *tert*-butyl chloride proceeds via an elimination mechanism. The lower reaction efficiencies relative to the proton-transfer reactions discussed earlier are due to transition states along the reaction coordinates. Transition states higher in energy than either a reactive intermediate or a dissociative intermediate effectively serve as "barriers" that must be overcome along the energy pathway of the reaction coordinate. The reaction coordinate plot for H^- + CH_3Cl is shown in Figure 3. Here, we consider proton-abstraction and substitution channels for the methyl chloride reaction. While both channels have transition-state barriers, the substitution channel has a lower barrier in addition to being more exothermic overall ($\Delta H = -91.4$ kcal mol^{-1} for the substitution versus -4.8 kcal mol^{-1} for the proton abstraction with respect to reactants). Additionally, we saw no evidence of the weakly bound CH_3^- anion. Similarly, we considered a substitution mechanism for the *tert*-butyl chloride reaction. We cannot distinguish between competing mechanisms for the *tert*-butyl chloride reaction since Cl^- is produced by both reactions. However, calculations predict the substitution reaction to have a higher transition-state energy barrier than the elimination reaction ($\Delta H = 10.7$ kcal mol^{-1} versus -8.4 kcal mol^{-1} at 298 K relative to reactant species). Therefore, we expect the substitution channel to have no contribution.

Prior measurement of the rate constant for the methyl chloride reaction was reported as $3.0 \pm 0.2 \times 10^{-9}$ cm^3 s^{-1} (mean value and precision of two measurements, with an overall accuracy of $\pm$20%) by Tanaka et al. (1976). Our determination for the methyl chloride S_N2 reaction is $2.5 \pm 0.1 \times 10^{-9}$ cm^3 s^{-1} (seven measurements) and $4.0 \pm 0.5 \times 10^{-9}$ cm^3 s^{-1} (nine measurements) for the *tert*-butyl chloride E2 reaction.

3.5. No Reaction

Some reactions in this study (H^- with diethyl ether, benzene, and molecular deuterium) exhibited little or no reactivity. We saw no decrease of reactant ion or formation of product ions in the reaction of hydride with diethyl ether. Typically, strong bases have been found to react prominently with ethers by elimination mechanisms (DePuy & Bierbaum 1981). However, calculations suggest that the elimination channel for the reaction of H^- with diethyl ether does not occur due to a barrier 5.4 kcal mol^{-1} higher in energy than the reactants along the reaction coordinate.

In reacting hydride with benzene, we noted a decrease in signal and made several attempts to measure a rate constant. In 14 attempts over the course of three days using two different high-purity benzene samples, we were left with an unreasonably low precision ($2 \pm 2 \times 10^{-11}$ cm^3 s^{-1}). Experimental and calculated enthalpies suggest that the reaction is thermoneutral, a possible cause of our problem. The presence of a relatively stable adduct could account for a slight decrease in the reactant ion signal. Bohme & Young (1971) studied the reaction of hydride with benzene in a series of bracketing experiments to determine electron affinities from thermal proton-transfer reactions. Their study was performed using a flowing-afterglow instrument, and generated H^- via electron ionization on NH_3 in helium. Their rate determination, $\geqslant 5 \times 10^{-11}$ cm^3 s^{-1}, resulted only in limiting values.

We observe only slight falloff in hydride signal intensity with the addition of D_2 (up to $\sim 2 \times 10^{12}$ cm^{-3}). The reaction, however, is thermoneutral, and hence, we see similar behavior to that in the reaction with benzene. Based on our observation, we set a limit to the reaction rate constant as $< 1 \times 10^{-11}$ cm^3 s^{-1}. However, our observations do show D^- production as H^- is depleted.

4. CONCLUSIONS

Table 1 is a compilation of our results which provide an increase in the accuracy of existing rate constants and a contribution of new rate constants. This study represents a chemical mapping of hydride reactivity with neutral species, many of which have been detected in the ISM. Experimental observations and contributions from ab initio calculations have accounted for a variety of reaction mechanisms and a range of reaction efficiencies.

We express our sincere gratitude for financial support from NASA, the NASA Graduate Student Researchers Program (GSRP), and the National Science Foundation (CHE-0647088). Additional support from the National Science Foundation comes from TeraGrid resources provided by the National Center for Supercomputing Applications.

REFERENCES

Betowski, D., Payzant, J. D., Mackay, G. I., & Bohme, D. K. 1975, Chem. Phys. Lett., 31, 321
Bierbaum, V. M. 2003, in The Encyclopedia of Mass Spectrometry, ed. P. B. Armentrout (Amsterdam: Elsevier), 940
Black, J. H. 1978, ApJ, 222, 125
Bohme, D. K., & Young, L. B. 1971, Can. J. Chem., 49, 2918
Chandrasekhar, S. 1944, ApJ, 100, 176
Chandrasekhar, S., & Breen, F. H. 1946, ApJ, 104, 430
DePuy, C. H., & Bierbaum, V. M. 1981, J. Am. Chem. Soc., 103, 5034
Dunkin, D. B., Fehsenfeld, F. C., & Ferguson, E. E. 1970, J. Chem. Phys., 53, 987
Fehsenfeld, F. C., Howard, C. J., & Ferguson, E. E. 1973, J. Chem. Phys., 58, 5841
Field, D. 2000, A&A, 362, 774
Gaussian 03: Frisch, M. J., et al. 2004, Gaussian, Inc., Wallingford, CT
Gioumousis, G., & Stevenson, D. P. 1958, J. Chem. Phys., 29, 294
Glover, S. C., Savin, D. W., & Jappson, A. -K. 2006, ApJ, 640, 553
Lide, D. R. 2008, CRC Handbook of Chemistry and Physics (89th ed.; Boca Raton, FL: CRC Press; Taylor & Francis Group)
Linstrom, P. J., & Mallard, W. G. (ed.) 2010, NIST Chemistry WebBook, NIST Standard Reference Database Number 69 (Gaithersburg, MD: NIST) 20899 (http://webbook.nist.gov)
Mackay, G. I., Betowski, L. D., Payzant, J. D., Schiff, H. I., & Bohme, D. K. 1976, J. Phys. Chem., 80, 2919
Mackay, G. I., Tanaka, K., & Bohme, D. K. 1977, Int. J. Mass Spec. Ion Proc., 24, 125
Martinez, O., Yang, Z., Betts, N. B., Snow, T. P., & Bierbaum, V. M. 2009, ApJ, 705, L172
Melton, C. E., & Neece, G. A. 1971, J. Am. Chem. Soc., 93, 6757
Münch, D. 1945, ApJ, 102, 385
NIST Computational Chemistry Comparison and Benchmark Database 2010, NIST Standard Reference Database Number 101, Release 15a, April 2010, ed. R. D. Johnson III (http://cccbdb.nist.gov/)
Ross, T., Baker, E. J., Snow, T. P., Destree, J. D., Rachford, B. L., Drosback, M. M., & Jensen, A. G. 2008, ApJ, 684, 358
Schmeltekopf, A. L., Fehsenfeld, F. C., & Ferguson, E. E. 1967, ApJ, 148, L155
Stockdale, J. A. D., Compton, R. N., & Reinhardt, P. W. 1968, Phys. Rev. Lett., 21, 664
Stockdale, J. A. D., Compton, R. N., & Reinhardt, P. W. 1969, Phys. Rev., 184, 81
Su, T., & Chesnavich, W. J. 1982, J. Chem. Phys., 76, 5183
Tanaka, K., Mackay, G. I., Payzant, J. D., & Bohme, D. K. 1976, Can. J. Chem., 54, 1643
Van Doren, J. M., Barlow, S. E., DePuy, C. H., & Bierbaum, V. M. 1987, Int. J. Mass Spectrom. Ion Proc., 81, 85
Wildt, R. 1939, ApJ, 90, 611